Cadherins at cell-autonomous membrane contacts control macropinocytosis

Peter J. B. Sabatini[1,2], Ming Zhang[2], Rosalind V. Silverman-Gavrila[1,2] and Michelle P. Bendeck[1,*]

[1]Department of Laboratory Medicine and Pathobiology, University of Toronto, Toronto, ON M5S 1A8, Canada
[2]Division of Cell and Molecular Biology, Toronto General Research Institute, University Health Network, Toronto, ON M5G 2C4, Canada
*Author for correspondence (michelle.bendeck@utoronto.ca)

Accepted 2 February 2011
Journal of Cell Science 124, 2013-2020

doi:10.1242/jcs.076901

Summary

Cadherins aggregate and stabilize cell–cell junctions through interactions with adjacent cells. In addition, N-cadherin and E-cadherin concentrate at free edges or at the lamellipodia of migrating cells and are found within large vesicles called macropinosomes, which develop from membrane ruffles. The binding properties of cadherins have not previously been associated with the localization of cadherins at membrane ruffles; however, we report that the dorsal, ventral and lateral membrane contacts that occur as a result of the overlap of membrane ruffles aggregate N-cadherin, and that both N-cadherin and E-cadherin promote macropinosome closure and fluid-phase uptake in macropinosomes. These data reveal a previously unsuspected function for cadherin-mediated cell–cell adhesion molecules in the closure of cell-autonomous membrane contacts at membrane ruffles, resulting in macropinocytosis.

Key words: Cadherins, Macropinocytosis, Membrane ruffling, Adhesion

Introduction

Cadherins are a family of homophilic cell–cell adhesion molecules that mediate actin-dependent contact between adjacent cells and regulate cell differentiation, proliferation and migration. N-cadherin is a pro-migratory cadherin subtype expressed on mesenchymal cells that promotes directional cell migration and polarity through intracellular signals at cell–cell junctions (Sabatini et al., 2008). By contrast, E-cadherin is expressed on epithelioid cells and is required to maintain a non-migratory polarized phenotype within these cells (Gibson and Perrimon, 2003). Despite these differences in regulatory roles, both N-cadherin and E-cadherin are also found concentrated at sites of membrane ruffles, such as the lamellipodia of migrating cells and the dorsal ruffles of growth-factor-stimulated cells (Bryant et al., 2007; Sharma and Henderson, 2007; Theisen et al., 2007).

Lamellipodia are specialized cellular structures that promote membrane protrusion. In these foot-like processes, mutual forces exerted within the assembling actin array at the leading edge of the cell drive membrane protrusion, while forcing retrograde flow of the actin array, the adjacent cell membrane and associated proteins (Pollard and Borisy, 2003). As a result of the protrusive and retractive dynamics, large fluid-filled endocytic vesicles called macropinosomes are formed in the lamellipodia and membrane ruffles (Swanson, 2008). Cadherins are concentrated at membrane protrusions and ruffles, and are internalized in macropinosomes, suggesting that they might be involved in macropinosome formation, although this has not been directly tested (Boguslavsky et al., 2007; Bryant et al., 2007; Sharma and Henderson, 2007). In addition, some proteins that associate with N-cadherin, including β-catenin, p120 catenin, platelet-derived growth factor receptor (PDGFR) and IQ-domain GTPase-activating protein 1, are also found at membrane ruffles, and are thought to recruit N-cadherin to these sites and enhance cell migration by promoting actin polymerization in lamellipodia (Boguslavsky et al., 2007; Sharma and Henderson, 2007; Theisen et al., 2007).

The data thus far suggest recruitment of cadherin towards these sites on the basis of interactions with molecules already known to be associated with lamellipodia and membrane ruffles. Cadherins, however, are cell–cell adhesion molecules that mediate their functions through homophilic interactions. Because lamellipodia are structures containing a large degree of membrane ruffling and overlapping membrane contacts, we propose that cadherins assist in aggregating the cell–cell adhesion molecules at these sites by using their homophilic binding properties. We have investigated the role of both E-cadherin- and N-cadherin-mediated adhesion as a potential mechanism not only in the recruitment of cadherins to the lamellipodia and membrane ruffles, but also as a regulator of functions occurring at these sites. Herein, we show that N-cadherin aggregates at cell-autonomous membrane contacts and that both E-cadherin and N-cadherin regulate the closure of macropinocytic vesicles.

Results

N-cadherin localizes to cell-autonomous membrane contacts in lamellipodia

An immortalized mouse aortic vascular smooth muscle cell line (MOVAS) (Afroze et al., 2003) was used to investigate the functions and fate of N-cadherin in lamellipodia. We scratch wounded MOVAS cells that were transfected with an N-cadherin–GFP plasmid (Mary et al., 2002) and visualized wound-edge cells expressing N-cadherin–GFP using fluorescence microscopy. Scratch wounding is commonly used to elicit local lamellipodia formation and directed cell migration to cover the wounded area.

Time-lapse confocal imaging of N-cadherin–GFP in lamellipodia revealed the appearance of punctate N-cadherin clusters in the lamellipodia that were not associated with classic cell–cell junctions (Fig. 1A; supplementary material Movie 1). Specifically, N-cadherin–GFP appeared at the neck of membrane invaginations only after autonomous membrane contact occurred to close the vesicular structure (Fig. 1A; supplementary material Movie 1).

Journal of Cell Science

To confirm the localization of N-cadherin to the neck of membrane invaginations, we labeled the surface of the cell with an Alexa-Fluor-647-tagged cholera toxin B-subunit (CTxB) membrane dye and found the formation of vesicular structures devoid of membrane (see asterisk in Fig. 1C), followed by N-cadherin–GFP appearing at the neck of the vesicle as the vesicle closes off (Fig. 1B, arrowhead; supplementary material Movie 2, right-most arrow). These results clearly demonstrate the capacity for N-cadherin to concentrate at sites of membrane overlap at the neck of membrane invaginations. These cell-autonomous membrane contacts are easily distinguished from N-cadherin associated with intercellular cell–cell junctions (Fig. 1B–D, arrows).

The appearance of N-cadherin at the leading edge was both punctate (Fig. 1E, arrow, Epi) and linear (Fig. 1E, arrowhead, Epi). To characterize the morphology of these structures, we employed total internal reflection fluorescence (TIRF) microscopy to determine whether the linear structures containing N-cadherin and visible by epifluorescence (Fig. 1E, arrowhead) were the result of membrane folding on the dorsal or ventral surface of the lamellipodia. TIRF imaging of N-cadherin–GFP revealed the formation of punctate clusters of N-cadherin–GFP at the ventral surface of the lamellipodia (Fig. 1F, arrow, TIRF). The linear structures were located on the dorsal surface because they could not be detected when imaged by TIRF (Fig. 1E,G, arrowheads), suggesting that they might represent membrane contacts in dorsal ruffles. These data suggest that N-cadherin concentrates at sites of dorsal ruffles and at sites where lateral membranes of the lamellipodia come together to form punctate N-cadherin–GFP clusters (Fig. 1H).

Retrograde flow of membrane-associated N-cadherin

Proteins, lipids and vesicles are transported away from the lamellipodia as a result of actin-dependent retrograde forces (Hu et al., 2007; Prigozhina and Waterman-Storer, 2004). In accord with the normal characteristics of proteins found in the lamellipodia, the punctate and linear N-cadherin clusters at the leading edge were also transported in a retrograde manner (Fig. 2A–E; supplementary material Movie 2).

N-cadherin associates with cholesterol-rich microdomains in the plasma membrane (Causeret et al., 2005); therefore, we analyzed the dynamics of N-cadherin–GFP and cholesterol-rich microdomains fluorescently labeled with CTxB using live-cell imaging (Fig. 2A–D). Kymographs show that CTxB was co-transported in a retrograde manner (Fig. 2B) with N-cadherin–GFP in the lamellipodia (Fig. 2C) and the velocities of N-cadherin–GFP and CTxB were similar (Fig. 2E).

N-cadherin promotes dextran uptake in lamellipodia

Large membrane invaginations and vesicles in the lamellipodia are characteristic of an endocytic process known as macropinocytosis, during which fluid-based uptake occurs at sites of increased membrane ruffling (Swanson, 2008). To determine whether there was fluid-based uptake in membrane ruffles of the lamellipodia, fluorescein isothiocyanate (FITC)-labeled dextran was added to the media to visualize fluid-phase internalization and then the cells were immunostained for N-cadherin. Fig. 2F shows the differential interference contrast (DIC) image of a MOVAS cell lamellipodium with a large vesicle internalized at the leading edge. Immunostaining revealed that endogenous N-cadherin (red) was found at the neck of a vesicle containing FITC–dextran (green) (Fig. 2G, arrow), consistent with the localization of N-cadherin–GFP shown in Fig. 1. Analysis of cells transfected with N-cadherin–GFP (Fig. 2H) revealed that aggregates of TRITC–dextran were found in vesicles in the lamellipodia (red) surrounded by N-

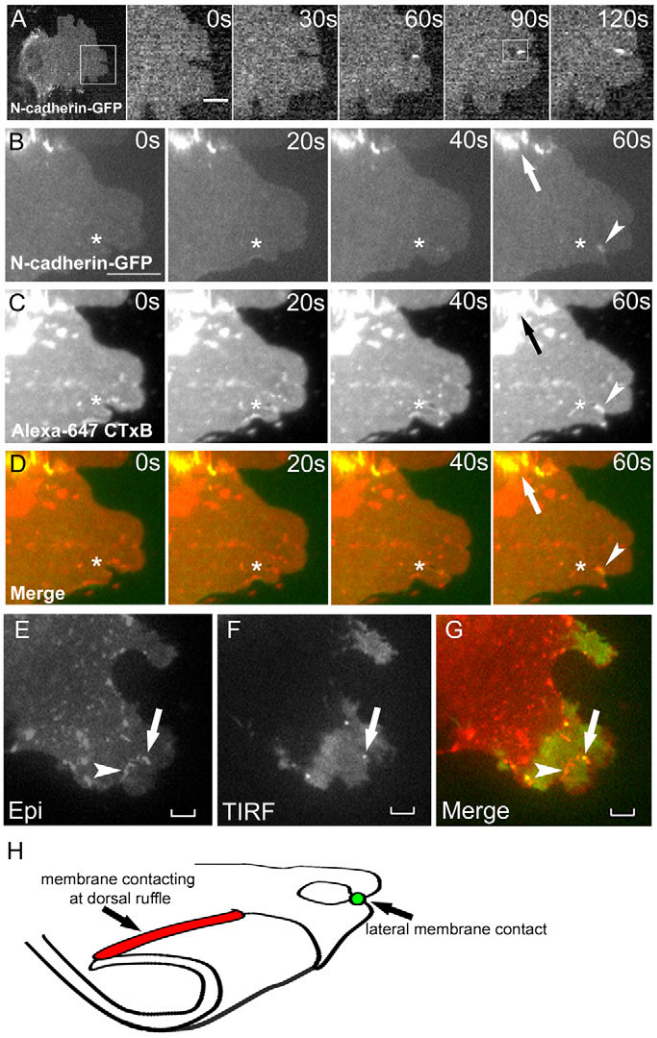

Fig. 1. N-cadherin appears at the neck of membrane inclusions in lamellipodia. (**A**) Fluorescent time-lapse images from a confocal microscope (supplementary material Movie 1) of a wound-edge MOVAS cell expressing N-cadherin–GFP at 4 hours following wounding. The region outlined in the white box represents the enlarged portion shown to the right as time-lapse images with the time displayed above. (**B–D**) Fluorescent time-lapse images from supplementary material Movie 2 of a wound-edge MOVAS cell expressing N-cadherin–GFP (B) and labeled with Alexa-Fluor-647–CTxB to visualize the membrane (C) and the merged images (D). The arrows point to N-cadherin–GFP at cell–cell junctions. The asterisks mark the newly formed vesicle in the lamellipodia. Notice the appearance of N-cadherin–GFP (arrowhead) (C) at the neck of the vesicle in the 60-second image. (**E–G**) Visualization of N-cadherin–GFP in the lamellipodia of wound-edge MOVAS cells 4 hours after wounding using TIRF microscopy to distinguish ventral from dorsal N-cadherin–GFP. Shown are the epifluorescent (Epi) (E), TIRF (F) and merged (G) images of a MOVAS cell expressing N-cadherin–GFP. The arrows point to ventrally localized N-cadherin–GFP and the arrowhead points to dorsally localized N-cadherin–GFP. (**H**) Schematic representing the linear dorsal distribution of N-cadherin (red) as a result of membrane ruffles folding back onto the plasma membrane and the punctate ventral localization of N-cadherin (green) due to the cell-autonomous contact of lateral membranes. Scale bars: 2 μm.

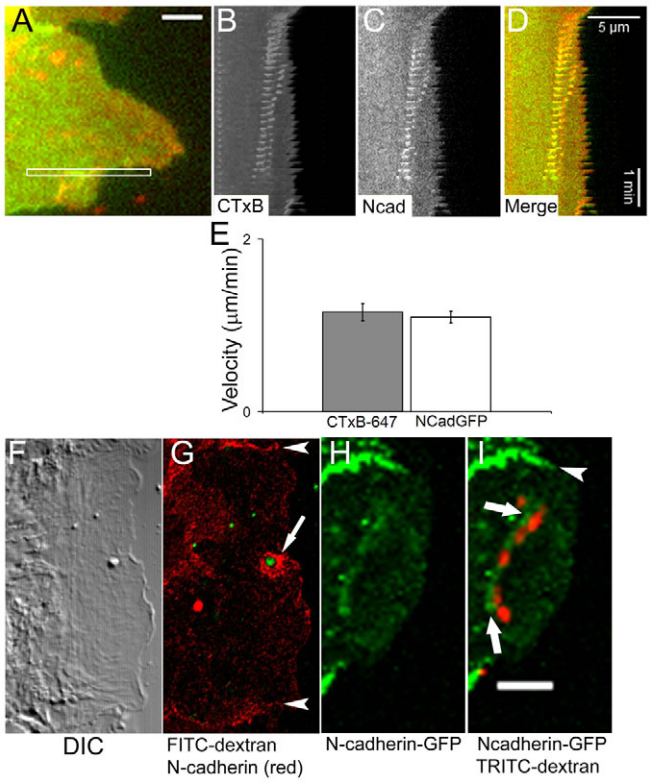

Fig. 2. Retrograde flow of N-cadherin with membrane. (**A–D**) Frame from live-cell imaging of a MOVAS cell expressing N-cadherin–GFP (supplementary material Movie 2) labeled with Alexa-Fluor-647–CTxB. (A) The white box defines the region prepared for kymographs (scale bar: 2 µm), which are displayed from left to right as Alexa-Fluor-647-conjugated CTxB (CTxB) (B) to label the membrane, N-cadherin–GFP (Ncad) (C) and the merged image of CTxB and N-cadherin–GFP (D) (horizontal marker: 5 µm; vertical marker: 1 minute). (**E**) Velocity (µm/min) of retrograde flow of CTxB–Alexa-Fluor-647 and N-cadherin–GFP in lamellipodia 4 hours after wounding confluent cultures of MOVAS cells. (**F**,**G**) DIC image (F) and confocal section (G) of a wound-edge MOVAS cell at 4 hours following wounding and treatment with FITC–dextran (green) for 1 hour prior to fixing and then immunostaining for N-cadherin (red). The arrowheads point to N-cadherin localized at cell–cell junctions and the arrow points to N-cadherin at the neck of a macropinosome. (**H**,**I**) MOVAS cells expressing N-cadherin–GFP (H) were incubated with TRITC–dextran (merged image, I) for 15 minutes at 1 hour after wounding, then fixed and visualized under a confocal microscope (scale bar: 5 µm). The arrowhead points to N-cadherin–GFP at cell–cell junctions and the arrows point to N-cadherin–GFP associated with dextran-containing vesicles in the lamellipodia.

cadherin–GFP (Fig. 2I, arrows) that were not associated with N-cadherin–GFP found at cell–cell junctions (Fig. 2I, arrowhead).

The localization of N-cadherin to the neck of macropinosomes suggests that it might participate in the sealing of budding vesicles at the plasma membrane and contribute to their internalization. To test this, the ability of cells to engulf FITC–dextran was measured in the presence of an N-cadherin antibody (Sigma, Clone GC-4) that interferes with the homophilic adhesion of N-cadherin. MOVAS cells were wounded, 1 hour later FITC–dextran was added for 5 minutes with either IgG or the N-cadherin antibody, and uptake was assessed. Specifically, FITC–dextran uptake was measured by plotting the percent area positive for FITC within cells located at the wound edge (area between the anterior nuclear membrane and the anterior tip of the plasma membrane of wound-edge cells) or within cells located in the confluent region posterior to the wound edge. MOVAS cells at wound edges internalized more FITC–dextran than cells in the confluent region of the monolayer, probably due to increased ruffling in wound-edge cells (Fig. 3A). Interfering with N-cadherin-mediated homophilic adhesion inhibited wound-induced uptake of FITC–dextran (Fig. 3B), but not dextran uptake in the confluent area compared with IgG-treated cells (Fig. 3F). These results were confirmed by also analyzing the percent of cells containing FITC–dextran (supplementary material Fig. S1). Interfering with N-cadherin adhesion inhibits cell migration and polarity (Sabatini et al., 2008), although membrane ruffling persisted in the presence of the N-cadherin blocking antibody (supplementary material Fig. S2).

Because the N-cadherin blocking antibody might stimulate signaling or interfere with other cadherins, we used a specific short-interfering RNA sequence to knockdown N-cadherin and quantified the uptake of FITC–dextran in wound-edge cells. Western blots revealed a 70% decrease in N-cadherin protein level following siRNA treatment (Fig. 3C). The knockdown of N-cadherin resulted in a significant decrease in FITC–dextran uptake in wound-edge cells (Fig. 3E) compared with cells transfected with a non-coding siRNA sequence (Fig. 3D). Quantification of these results, expressed as the percentage cell area positive for dextran, is shown in Fig. 3F and expressed as the percentage of cells containing dextran is shown in supplementary material Fig. S1. Collectively, our data show that N-cadherin promotes fluid-based uptake of dextran at the ruffles of migrating wound-edge cells by sealing macropinosomes.

N-cadherin promotes macropinocytosis in PDGF-BB stimulated cells

Growth factors enhance macropinocytosis by inducing intracellular signals that promote membrane ruffling. Interestingly, E-cadherin and N-cadherin are both internalized into macropinosomes following growth factor stimulation (Bryant et al., 2007; Sharma and Henderson, 2007), suggesting a link between cadherin function and growth factor stimulation of macropinocytosis. Recent studies have shown that the PDGFR localizes to the leading edge of migrating cells and recruits N-cadherin to the lamellipodia (Theisen et al., 2007). Moreover, PDGF signaling stimulates vascular smooth muscle cell migration and proliferation (Jawien et al., 1992). Thus, a role for PDGF signaling in controlling N-cadherin-mediated macropinocytosis is of particular relevance to migration in vascular smooth muscle cells.

Macropinocytosis requires both actin dynamics and phosphatidylinositol 3-kinase (PI3K)-dependent signals to induce membrane ruffling and internalization of macropinosomes (Koivusalo et al., 2010). To verify that MOVAS cells engulf dextran into macropinosomes, PDGF-BB (100 ng/ml) was added to serum-starved subconfluent MOVAS cells to stimulate membrane ruffling and FITC–dextran uptake was measured in the presence or absence of the actin inhibitor latrunculin B (100 nM) or the PI3K inhibitor LY294002 (10 µM). The uptake of FITC–dextran was measured by tracing the perimeter of the cells and quantifying the percentage of FITC–dextran-positive pixels above background levels within the cell following 15 minutes incubation with PDGF-BB and FITC–dextran.

PDGF-BB-stimulated actin-rich membrane ruffles in MOVAS cells (compare Fig. 4A, untreated cells, with 4B, PDGF-treated

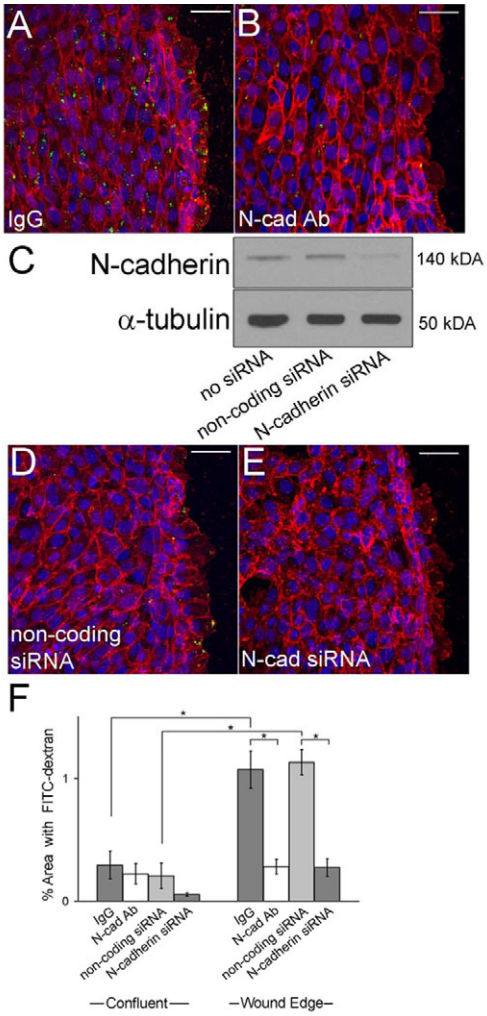

Fig. 3. N-cadherin promotes macropinocytosis in wound-edge cells. (**A**) Confocal micrograph of MOVAS cells at the wound edge treated with a non-specific IgG antibody and FITC–dextran (green) for 5 minutes, and labeled with CTxB–Alexa–Fluor-647 (red) to visualize the cell membrane and Hoechst (blue) to visualize the nuclei. (**B**) As in A, except an N-cadherin blocking antibody was added when FITC–dextran was added to the wounded cells. Scale bars: 50 µm. (**C**) Western blot for N-cadherin in MOVAS cells that were either left untreated (no siRNA) or transfected with non-coding siRNA or siRNA against N-cadherin. (**D**) Confocal micrograph of MOVAS cells at the wound edge that were transfected with a non-coding siRNA, wounded, then 1 hour later incubated with FITC–dextran for 5 minutes, and labeled with CTxB–Alexa-Fluor-647 to visualize the cell membrane and Hoechst to visualize the nuclei. (**E**) As in D, except cells were transfected with siRNA against N-cadherin to knockdown N-cadherin. Scale bars: 50 µm (**F**) Graph representing the percentage of confluent and wound-edge area that is positive for FITC–dextran. The number of pixels above background level was calculated and expressed as a percentage of the total area between the anterior nuclear membrane and the leading edge of wound-edge cells (wound edge) or in the region posterior to the wound edge (confluent area). All data and images represent the results of at least three independent experiments (**P*<0.05). Data are means±s.e.

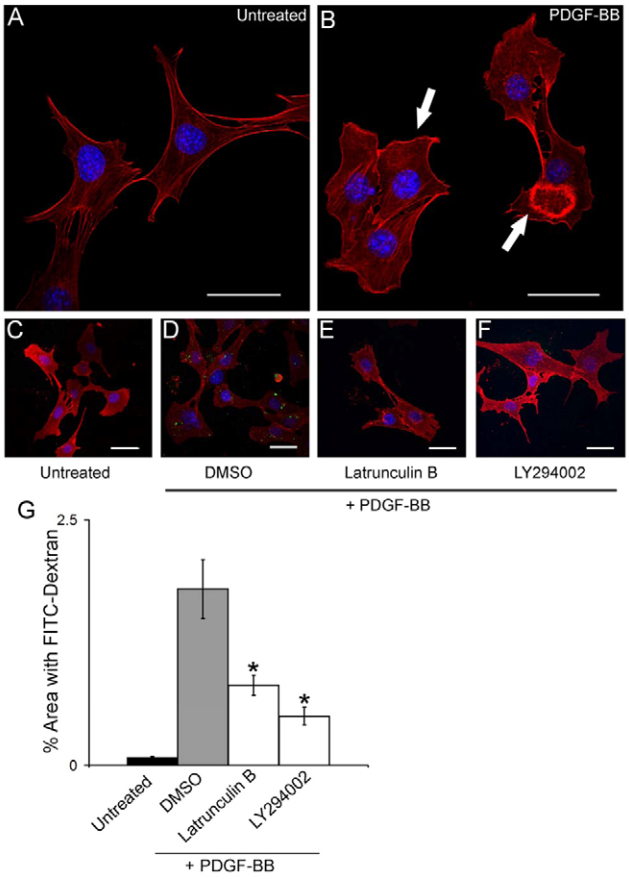

Fig. 4. PDGF-BB stimulates macropinocytosis in MOVAS cells. (**A**) Confocal micrograph of serum-starved MOVAS cells labeled with Rhodamine-phalloidin (red) to visualize the actin network and Hoechst to visualize the nucleus (blue). (**B**) Confocal micrograph of PDGF-BB-treated MOVAS cells labeled with Rhodamine-phalloidin. The arrows point to distinct membrane ruffles that are associated with actin fibers. (**C**) Serum-starved (untreated) MOVAS cells incubated with FITC–dextran (green) and labeled with CTxB–Alexa-Fluor-647 (red) to visualize the cell membrane and Hoechst (blue) to visualize the nucleus. (**D**) As in C, except cells were stimulated with PDGF-BB and DMSO. (**E**) Micrograph displaying MOVAS cells that were pre-incubated with latrunculin B to disrupt the actin network before PDGF-BB and FITC–dextran addition. No FITC–dextran uptake was observed under these conditions. (**F**) As in E, except cells were pre-incubated with LY294002 to inhibit PI3K. As with latrunculin B treatment, no FITC–dextran uptake was observed when PI3K was inhibited. Scale bars: 50 µm. (**G**) Graph representing the percent area that is positive for FITC–dextran above background levels, measured by tracing out the periphery of each cell and calculating the percent area positive for FITC–dextran. All data and images represent the results of at least three independent experiments (**P*<0.05 compared to DMSO treatment). Data are means±s.e.

cells). PDGF-BB also stimulated the uptake and translocation of FITC–dextran to the perinuclear area of the cell (Fig. 4D); this was not observed in the absence of PDGF-BB (Fig. 4C). Pre-incubation with either latrunculin B (Fig. 4E) or LY294002 (Fig. 4F) significantly abrogated dextran uptake in PDGF-BB-stimulated MOVAS cells. Quantification of these results expressed as the percent cell area positive for dextran is shown in Fig. 4G (and expressed as the percentage of cells containing dextran in supplementary material Fig. S3A). These data demonstrate that growth factor stimulation of membrane ruffling in MOVAS cells induces macropinocytosis

We next measured the ability of PDGF-BB-stimulated MOVAS cells to engulf FITC–dextran into macropinosomes following disruption of N-cadherin. Interfering with homophilic adhesion using the N-cadherin antibody or treatment with siRNA to

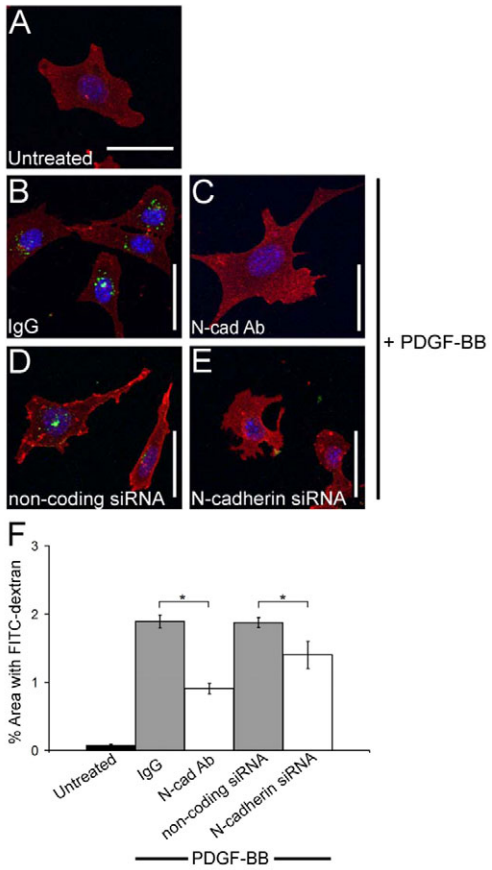

Fig. 5. N-cadherin promotes macropinocytosis in PDGF-BB-stimulated subconfluent cells. (**A–E**) Subconfluent serum-starved MOVAS cell incubated with FITC–dextran for 15 minutes in serum-free DMEM (A) and treated with 100 ng/ml PDGF-BB and IgG (B) or anti-N-cadherin antibody (C), or transfected with a non-coding siRNA (D) or an siRNA against N-cadherin (E). All cells were labeled with Alexa-Fluor-647–CTxB to visualize the cell membrane and Hoechst as a nuclear counterstain. Scale bars: 50 µm. (**F**) Graph representing the percent area that is positive for FITC–dextran above background levels, measured by tracing out the periphery of each cell and calculating the percent area positive for FITC–dextran. All data and images represent the results of at least three independent experiments (**P*<0.05). Data are means±s.e.

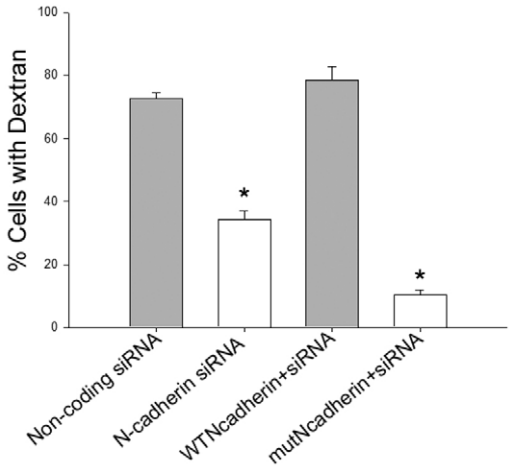

Fig. 6. The extracellular homophilic adhesion domain of N-cadherin is required for macropinocytosis. Graph representing the percentage of cells exhibiting TRITC–dextran uptake. Cells were transfected with non-coding siRNA or siRNA against N-cadherin, which significantly decreased dextran uptake (compare two bars on the left). Dextran uptake was restored after transfection with wild-type N-cadherin, but not after transfection with a truncated mutant of N-cadherin lacking the homophilic adhesion domain (compare two bars on the right). All data represent the results of at least three experiments (**P*<0.05). Data are means + s.e.

knockdown N-cadherin attenuated the uptake of FITC–dextran in PDGF-BB-stimulated cells (Fig. 5). Quantification of the percent cell area positive for FITC–dextran showed a significant loss of FITC–dextran uptake following treatment with N-cadherin antibody or N-cadherin siRNA (Fig. 5F), as did measurement of the percentage of cells containing dextran (supplementary material Fig. S3B).

Homophilic adhesion is mediated by the extracellular domain of N-cadherin (Kintner, 1992). We transfected subconfluent cells with plasmids encoding either wild-type N-cadherin or a dominant-negative N-cadherin mutant with a truncation deleting the extracellular domain (Cheng et al., 2000) to attempt to rescue the siRNA-transfected cells and restore dextran uptake. The siRNA does not affect expression of the N-cadherin plasmids. siRNA targeting of N-cadherin significantly reduced TRITC–dextran uptake compared with a non-coding siRNA control (Fig. 6). Transfection with the wild-type N-cadherin restored dextran uptake to a level comparable to that of cells transfected with non-coding siRNA (Fig. 6). By contrast, transfection of the mutant N-cadherin did not restore dextran uptake following the siRNA inhibition (Fig. 6). Considering the localization of N-cadherin to the neck of large vesicles at membrane ruffles and our finding that the extracellular homophilic adhesion domain of N-cadherin is required for dextran uptake, our data suggest that N-cadherin functions in sealing cell-autonomous membrane contacts during macropinocytosis.

E-cadherin promotes macropinocytosis in EGF-stimulated A431 cells

E-cadherin is also found in macropinosomes following epidermal growth factor (EGF) stimulation of epithelial cells (Bryant et al., 2007). To investigate the role of E-cadherin in macropinocytosis, we used A431 cells that express E-cadherin and rapidly form actin-rich membrane ruffles and macropinosomes after stimulation with EGF (Koivusalo et al., 2010). A431 cells were serum starved and then treated with 100 ng/ml EGF and tetramethyl Rhodamine (TMR)–dextran (0.25 mg/ml) to visualize macropinocytosis. When E-cadherin was disrupted either with an E-cadherin blocking antibody or by knocking down E-cadherin with siRNA (Fig. 7A), dextran uptake was impaired compared with that of cells treated with IgG or non-coding siRNA (Fig. 7B,C). These data indicate that E-cadherin is important for the uptake of dextran into macropinosomes and their closure, and imply a general role for cadherins in the macropinocytic process, at least in these two different cell types.

Discussion

Cadherins are crucial to tissue morphogenesis and stability through their functions as cell–cell adhesion molecules; however, these experiments establish a novel role for cadherins outside

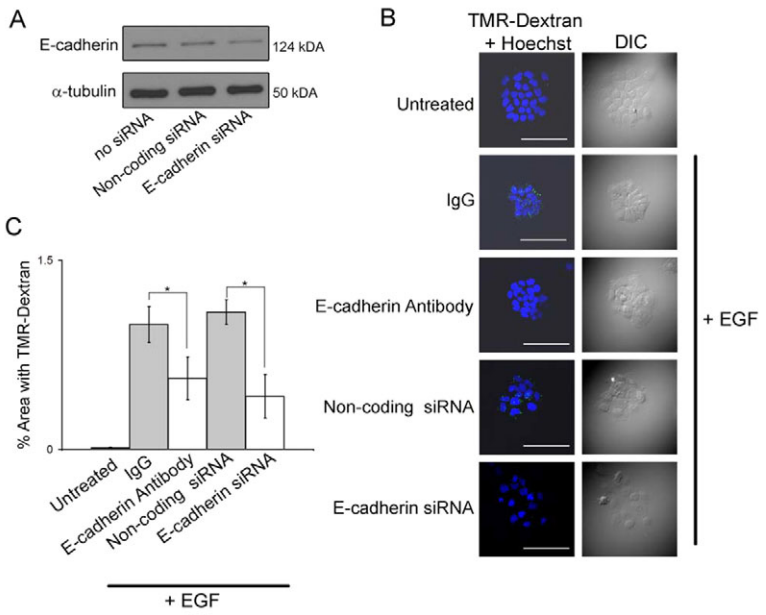

Fig. 7. E-cadherin promotes macropinocytosis in EGF-stimulated A431 cells. (**A**) Western blot for E-cadherin in A431 cells that were either left untreated (no siRNA) or transfected with non-coding siRNA or siRNA encoding E-cadherin. Approximately 60% knockdown of E-cadherin was achieved. (**B**) Confocal micrographs of A431 cells incubated with TMR–dextran (green) and labeled with Hoechst (blue) to visualize the nucleus. The cells were either serum starved (untreated) or treated with EGF for 10 minutes in the presence of IgG, E-cadherin blocking antibody, non-coding siRNA or E-cadherin-specific siRNA. The arrows show dextran-positive vesicles within A431 cells. Scale bars: 50 µm. (**C**) Graph representing the percent area that is positive for TMR–dextran above background levels, measured by tracing out the periphery of each colony of A431 cells and calculating the percent area positive for TMR–dextran. All data and images represent the results of at least three independent experiments (**P*<0.05). Data are means ± s.e.

that of the classic intercellular adhesions. We demonstrate that, at sites of cell-autonomous membrane overlap in areas of membrane ruffling, cadherins aggregate and, by mediating homophilic membrane adhesions, might assist in the closure of vesicles called macropinosomes. Therefore, we propose that cadherins might also mediate these functions in isolated single cells or cells at the free edges of tissues that arise during gastrulation or wound healing.

Membrane ruffling and cadherins control cell motility; therefore, one implication of our findings is that the sealing of cell-autonomous membrane contacts by cadherins in the lamellipodia is important to migratory processes. A consequence of this is the consolidation of multiple membrane protrusions into a single lamellipodium. Polarized and spreading cells are able to maintain a uniform lamellipodium, despite the stochastic nature of the protrusive and retractive forces and differences in adhesion to the substrate. One interpretation of our findings is that, by binding two protrusions and promoting their fusion, N-cadherin might participate in the maintenance of uniform lamellipodial morphology in motile cells. Therefore, our current data identify a possible new function for N-cadherin in promoting polarized cell migration by regulating the uniformity of the lamellipodia. Our studies were limited to short-term experimental conditions (5–15 minutes) and it will be important to study the long-term consequences of N-cadherin disruption on membrane morphology, particularly in situations of highly active membrane dynamics.

Experiments with a truncated N-cadherin lacking the extracellular domain revealed that homophilic N-cadherin binding was required to promote uptake of dextran into cells. This suggests that, in addition to maintaining stable intracellular adhesions, N-cadherin can mediate more transient cell-autonomous membrane contacts that close macropinocytotic vesicles. This is a new description of function for N-cadherin, mediated by physical binding interactions and not signaling by the receptor.

Our findings might also be pertinent to processes of innate immunity. Immature dendritic cells utilize macropinocytosis to constitutively sample the extracellular space in search for foreign antigens that are later presented on the surface of mature dendritic cells. A role for cadherins in this process has not been investigated. However, our data show that cadherins are required for macropinocytosis; therefore, they might be important in promoting the immune functions of immature dendritic cells. Interfering with cadherin function on antigen-presenting cells could limit the immunity against numerous invasive pathogens (Norbury, 2006).

We show how cadherins are involved in the internalization of macropinosomes on cells, as we are interested in actively protruding cell membranes; however, all forms of endocytosis rely on similarly shaped membrane curvature. Thus, we cannot exclude the possibility that cadherins also assist in the sealing of phagosomes as well as in clathrin-dependent and -independent modes of endocytosis. It will be interesting to examine the localization of cadherins within these smaller and more regulated forms of endocytosis.

To conclude, we have demonstrated that membrane ruffles and the lamellipodia create sites of cadherin-dependent adhesion, as lateral, dorsal or ventral membranes make cell-autonomous contacts that initiate the internalization of macropinosomes. Cell-autonomous membrane contacts resulting from membrane ruffling mediated by growth factors and wound healing are thus highly populated with a functional subset of cadherins that control processes beyond the classic regulation of intercellular adhesions.

Materials and Methods

Cell culture and reagents

The MOVAS smooth muscle cell line was kindly provided by Mansoor Husain (Toronto, Canada) and the A431 cell line was a gift from Sergio Grinstein (Toronto, Canada). The cells were grown in DMEM supplemented with 10% calf serum and 1% penicillin/streptomycin. To stimulate lamellipodia formation, smooth muscle cells were plated on glass cover slips and post-confluent cultures were scratch wounded by dragging a 200 µl pipette tip across the bottom of the plate. All other experiments were performed under subconfluent conditions.

Immunofluorescence staining

Cells were fixed with 4% paraformaldehyde for 20 minutes and permeabilized with 0.2% Triton X-100 for 5 minutes. Anti-N-cadherin antibody [1:50; BD Biosciences (673610920), Mississauga, Canada] was used with a CY3-conjugated secondary antibody (1:50; Jackson ImmunoResearch Laboratories, West Grove, PA). All samples were visualized using an Olympus FV1000 laser-scanning confocal microscope with a 40× or 60× oil-immersion (NA=1.4) objective. TIRF images were captured using a Nikon TE2000 microscope equipped with Nikon TIRF II and a 60× oil immersion TIRF lens. Basal N-cadherin–GFP was excited with a 488 nm argon laser.

Plasmids and transfections

Plasmids encoding N-cadherin–GFP were from Cecile Gauthier-Rouviere (Paris, France) (Mary et al., 2002). Plasmids were transformed into competent *Escherichia coli* at 42°C, grown in kanamycin (50 μg/ml) and a Qiagen mini-prep kit was used to purify the plasmid. Subconfluent smooth muscle cells were transfected with 4 μg of plasmid DNA containing 30 μl of Effectene and 24 μl of Enhancer provided by the Effectene transfection kit (Qiagen). After 48 hours, cells were wounded and either fixed with 4% paraformaldehyde or live cells were transferred to the microscope for fluorescence imaging. A mutant plasmid with the extracellular domain of N-cadherin deleted (mutNcadherin) was obtained from Roberto Civitelli (St Louis, MO) (Cheng et al., 2000).

Live-cell imaging

To analyze cell fluorescence, videos were captured in a temperature-controlled chamber at 37°C using a Nikon TE2000 or Olympus FV1000 scanning confocal microscope under a 60× (NA=1.4) oil-immersion objective equipped with DIC and 488 nm, 543 nm or 620 nm filter cubes. Images were captured using a Hamamatsu Photonics camera (C4742-95-12ER) controlled by Simple PCI software (Hamamatsu Cooperation, Sewickley, PA) for the TE2000 microscope. All image analysis was done using Simple PCI and Image J (NIH) software, and is described in detail below.

Analysis of transport of cholesterol-rich microdomains and N-cadherin–GFP in lamellipodia

Post-confluent MOVAS cells were transfected with N-cadherin–GFP and were incubated in Hank's buffered saline solution (HBSS, pH 7.4) containing essential and nonessential MEM amino acids (GIBCO, Invitrogen), 2 mM glutamine, 1 mM sodium pyruvate and 1% calf serum (to reduce autofluorescence during imaging) for 24 hours and then wounded. Four hours later, 1 μg/ml Alexa-Fluor-647-labeled CTxB (Invitrogen, C3478) was added to the cells on ice for 5 minutes, then rinsed in HBSS three times and visualized for up to 1 hour at 37°C at 0.1 frames/second.

Kymographs and determination of the velocity of retrograde flow

Velocities of N-cadherin–GFP or CTxB in the lamellipodia were determined from 10-minute movies by cropping an ~5 μm × 0.5 μm region of the lamellipodium orthogonal to the wound edge and displaying temporal changes in the image as a kymograph. Velocity was determined from the slope of the line(s) created by the flow of fluorescent label and expressed as mean velocities from all moving particles from three independent movies (see Fig. 2E). A one-way ANOVA was followed by a Newman–Keuls comparison to determine statistical significance ($P<0.05$).

We also prepared kymographs to assess membrane ruffling. Kymographs were prepared from phase-contrast live-cell imaging of MOVAS cells migrating at the edge of a wound made in the confluent monolayer. Ruffles were evident as dark phase-dense ridges at the leading edge of lamellipodia. Kymographs were made by drawing a three-pixel-wide line through the lamellipodium of cells treated with IgG or anti-N-cadherin antibody, from movies collected over a one-hour period, starting one hour after wounding. The average intensity over the three pixels was calculated using Nikon Elements NIS software.

siRNA knockdown

Transfection of MOVAS cells with siRNA was done using the Effectene transfection kit as described above (Qiagen) and 200 nM of either N-cadherin-specific siRNA (GGAUGUGCACGAAGGACAGtt, siRNA ID 60629, Applied Biosystems, CA) or a non-coding negative control siRNA (AM4611, Applied Biosystems). MOVAS cells were plated either at high density for the wound experiments (1.5×10^6 cells) or at low density (1.0×10^5 cells) for the PDGF experiments. Twenty-four hours after plating, cells were incubated with the N-cadherin-specific siRNA or the non-coding siRNA complexed with Effectene for 8 hours, then rinsed in either 10% calf serum (wound experiments) or serum-free media (PDGF experiments) for 16 hours.

To knockdown E-cadherin in A431 cells, Lipofectamine RNAiMAX (Invitrogen) was used as directed by plating approximately 5000 cells and 72 hours later incubating 5 μl of Lipofectamine RNAiMAX with 25 nM of either E-cadherin-specific siRNA (GGACAGCCUAUUUUUCCCUtt, siRNA ID 42832, Applied Biosystems) or a non-coding control siRNA (Applied Biosystems) for up to 16 hours. The cells were then rinsed in serum-free DMEM for 4 hours prior to EGF stimulation.

Both N-cadherin and E-cadherin levels were measured by collecting cell lysates in SDS lysis buffer and boiling them for 10 minutes, then loading 5 μg of protein onto a 10% polyacrylamide gel and transferring to a PVDF membrane for western blotting. Anti-N-cadherin (1:5000, BD Transduction), anti-E-cadherin [1:10,000, Calbiochem (205601), Darmstadt, Germany], anti-α-tubulin [1:10,000, Sigma (T9026)] and anti-mouse HRP (1:10,000, Amersham Bioscience, Baie d'Urfe, Canada) antibodies were used to visualize the bands. Densitometry was performed using ImageJ software to quantify the level of knockdown achieved using α-tubulin as a loading control.

Dextran uptake in wound-edge cells

To visualize internalized vesicles, 2 mg/ml of 70 kDa FITC [Sigma (46945)] or TRITC–dextran [Sigma (T1162)] was added 4 hours after wounding post-confluent MOVAS cells and incubated at 37°C for 1 hour. Cells were then fixed and stained for N-cadherin or fixed to visualize N-cadherin–GFP and analyzed using a FV1000 laser scanning confocal microscope.

To quantify the level of FITC–dextran uptake in wounded confluent monolayers, MOVAS cells were wounded and 1 hour later FITC–dextran was added for 5 minutes with either 50 μg/ml of a monoclonal anti-N-cadherin blocking antibody [clone GC-4, Sigma (C2542)] that binds to the extracellular domain of N-cadherin to interfere with N-cadherin-mediated homophilic binding or 50 μg/ml of a non-specific IgG (Sigma).

The cells were then fixed and stained with Hoechst 33342 (2 μg/ml) to visualize the nuclei and CTxB–Alexa-Fluor-647 (1 μg/ml) to label the cell membrane. The N-cadherin-specific or non-coding siRNAs were transfected into the cells 8 hours prior to wounding.

Images at wound edges were captured with a FV1000 laser scanning confocal microscope and a 40× oil-immersion objective, then analyzed with ImageJ software. The number of pixels above the background level at 488 nm excitation wavelength was calculated by tracing out the region between the anterior-most nuclear membrane and the leading edge of the cell, and was expressed as the percent area positive for FITC–dextran. A 7182 μm^2 box (approximate size of wound edge area) was traced out behind the wound edge to measure the level of dextran uptake in the confluent layer. A second measurement of the percentage of cells containing dextran was also calculated. A one-way ANOVA was followed by a Newman–Keuls comparison to determine statistical significance ($P<0.05$).

Growth factor stimulation of dextran uptake

Subconfluent MOVAS cells were incubated in serum-free DMEM for up to 24 hours, then treated for 15 minutes with 100 ng/ml PDGF-BB [Sigma (P4056)] and the non-specific IgG antibody or the N-cadherin blocking antibody, or transfected with the N-cadherin-specific siRNA or non-coding siRNA. In the case of actin and PI3K disruption, the cells were pre-incubated for 30 minutes with 10 μM LY294002 [Sigma (L9908)] or 100 nM latrunculin B [Sigma (L5288)] prior to adding PDGF-BB and FITC–dextran.

Following FITC–dextran administration, cells were fixed in paraformaldehyde, then prepared and imaged as described above. Analysis of the uptake of dextran was done by tracing out the perimeter of each cell and determining the number of pixels above background (488 nm), expressed as percent area positive for FITC–dextran. Approximately 75 cells were analyzed per experiment and the average of three experiments was used to graph the percent area positive. A second measurement of the percentage of cells containing dextran was also calculated. A one-way ANOVA was followed by a Newman–Keuls comparison to determine statistical significance ($P<0.05$).

A431 cells were plated at subconfluence and allowed to grow for 72 hours. Cells were then incubated for 4–16 hours in serum-free media and 100 ng/ml of EGF [Invitrogen (E3476)] was added to the cells with 0.25 mg/ml of 70 kDa TMR–dextran [Invitrogen (D1818)] for 10 minutes. In addition, the cells were either incubated with 10 μg/ml of an anti-E-cadherin blocking antibody (Calbiochem) or 10 μg/ml of a non-specific IgG antibody (Sigma), or transfected with the E-cadherin-specific siRNA or the non-coding siRNA sequences, as described above.

To quantify TMR–dextran uptake, A431 cells were fixed and prepared as with the MOVAS cells. The colonies of cells were traced out using the DIC images and the level of TMR–dextran fluorescence above background levels (543 nm) was calculated. Approximately 150 cells were analyzed per experiment and the average of three experiments was used to graph the percent area positive. A one-way ANOVA was followed by a Newman–Keuls comparison to determine statistical significance ($P<0.05$).

siRNA rescue experiments

MOVAS cells were plated in six-well plates at subconfluent density. Four hours after plating, cells were serum starved for 12 hours, then incubated with 200 nM N-cadherin-specific siRNA or non-coding siRNA complexed with Effectene, as described above. Four hours later, cells were transfected with plasmid encoding wild-type N-cadherin–GFP (0.5 μg/well) or a mutant plasmid with the extracellular domain of N-cadherin deleted (mutNcadherin) (0.5 μg/well) using Effectene (10 μl/well). After 4 hours, the cells were stimulated with 100 ng/ml PDGF-BB and incubated with TRITC–dextran (2ng/ml) for 15 minutes at 37°C. Cells were fixed and stained with Hoescht as described above, and cells were counted to determine the percentage of cells containing dextran. At least 75 cells were counted for each experimental condition and the experiments were repeated three times.

We thank C. Gauthier-Rouviere (Paris, France) for providing the N-cadherin–GFP plasmid, R. Civitelli (St Louis, MO) for providing the mutant extracellular domain truncated N-cadherin plasmid, S. Grinstein for providing the A431 cell line and M. Husain for the MOVAS cells. We also acknowledge M. Koivusalo and S. Grinstein for their helpful discussions. This work was funded by the Heart and Stroke Foundation

of Ontario (grant T6084) to M.P.B. P.J.B.S. is the recipient of a Canadian Institute for Health Research Doctoral Canada Graduate Scholarship and M.P.B. was a Career Investigator of the Heart and Stroke Foundation of Ontario. We also thank B. L. Langille for his valuable insight into this project.

Supplementary material available online at
http://jcs.biologists.org/cgi/content/full/124/12/2013/DC1

References

Afroze, T., Yang, L. L., Wang, C. S., Gros, R., Kalair, W., Hoque, A. N., Mungrue, I. N., Zhu, Z. P. and Husain, M. (2003). Calcineurin-independent regulation of plasma membrane Ca^{2+} ATPase-4 in the vascular smooth muscle cell cycle. *Am. J. Physiol. Cell Physiol.* **285**, C88-C95.

Boguslavsky, S., Grosheva, I., Landau, E., Shtutman, M., Cohen, M., Arnold, K., Feinstein, E., Geiger, B. and Bershadsky, A. (2007). p120 catenin regulates lamellipodial dynamics and cell adhesion in cooperation with cortactin. *Proc. Natl. Acad. Sci. USA* **104**, 10882-10887.

Bryant, D. M., Kerr, M. C., Hammond, L. A., Joseph, S. R., Mostov, K. E., Teasdale, R. D. and Stow, J. L. (2007). EGF induces macropinocytosis and SNX1-modulated recycling of E-cadherin. *J. Cell Sci.* **120**, 1818-1828.

Causeret, M., Taulet, N., Comunale, F., Favard, C. and Gauthier-Rouviere, C. (2005). N-cadherin association with lipid rafts regulates its dynamic assembly at cell-cell junctions in C2C12 myoblasts. *Mol. Biol. Cell* **16**, 2168-2180.

Cheng, S. L., Shin, C. S., Towler, D. A. and Civitelli, R. (2000). A dominant negative cadherin inhibits osteoblast differentiation. *J. Bone Miner. Res.* **15**, 2362-2370.

Gibson, M. C. and Perrimon, N. (2003). Apicobasal polarization: epithelial form and function. *Curr. Opin. Cell Biol.* **15**, 747-752.

Hu, K., Ji, L., Applegate, K. T., Danuser, G. and Waterman-Storer, C. M. (2007). Differential transmission of actin motion within focal adhesions. *Science* **315**, 111-115.

Jawien, A., Bowen-Pope, D. F., Lindner, V., Schwartz, S. M. and Clowes, A. W. (1992). Platelet-derived growth factor promotes smooth muscle migration and intimal thickening in a rat model of balloon angioplasty. *J. Clin. Invest.* **89**, 507-511.

Kintner, C. (1992). Regulation of embryonic cell adhesion by the cadherin cytoplasmic domain. *Cell* **69**, 225-236.

Koivusalo, M., Welch, C., Hayashi, H., Scott, C. C., Kim, M., Alexander, T., Touret, N., Hahn, K. M. and Grinstein, S. (2010). Amiloride inhibits macropinocytosis by lowering submembranous pH and preventing Rac1 and Cdc42 signaling. *J. Cell Biol.* **188**, 547-563.

Mary, S., Charrasse, S., Meriane, M., Comunale, F., Travo, P., Blangy, A. and Gauthier-Rouviere, C. (2002). Biogenesis of N-cadherin-dependent cell-cell contacts in living fibroblasts is a microtubule-dependent kinesin-driven mechanism. *Mol. Biol. Cell* **13**, 285-301.

Norbury, C. C. (2006). Drinking a lot is good for dendritic cells. *Immunology* **117**, 443-451.

Pollard, T. D. and Borisy, G. G. (2003). Cellular motility driven by assembly and disassembly of actin filaments. *Cell* **112**, 453-465.

Prigozhina, N. L. and Waterman-Storer, C. M. (2004). Protein kinase D-mediated anterograde membrane trafficking is required for fibroblast motility. *Curr. Biol.* **14**, 88-98.

Sabatini, P. J. B., Zhang, M., Silverman-Gavrila, R., Bendeck, M. P. and Langille, B. L. (2008). Homotypic and endothelial cell adhesions via N-cadherin determine polarity and regulate migration of vascular smooth muscle cells. *Circ. Res.* **103**, 405-412.

Sharma, M. and Henderson, B. R. (2007). IQ-domain GTPase-activating protein 1 regulates beta-catenin at membrane ruffles and its role in macropinocytosis of N-cadherin and adenomatous polyposis coli. *J. Biol. Chem.* **282**, 8545-8556.

Swanson, J. A. (2008). Shaping cups into phagosomes and macropinosomes. *Nat. Rev. Mol. Cell Biol.* **9**, 639-649.

Theisen, C. S., Wahl, J. K., Johnson, K. R. and Wheelock, M. J. (2007). NHERF links the N-cadherin/catenin complex to the platelet-derived growth factor receptor to modulate the actin cytoskeleton and regulate cell motility. *Mol. Biol. Cell* **18**, 1220-1232.